Six-Rowed Spike3 (VRS3) Is a Histone Demethylase That Controls Lateral Spikelet Development in Barley[1][OPEN]

G. Wilma van Esse,[a,b,c,2,3] Agatha Walla,[a,b,c,2] Andreas Finke,[a] Maarten Koornneef,[a,d] Ales Pecinka,[a] and Maria von Korff[a,b,c,4]

[a]Department of Plant Breeding and Genetics, Max Planck Institute for Plant Breeding Research, 50829 Köln, Germany
[b]Institute for Plant Genetics, Heinrich-Heine-Universität Düsseldorf, 40225 Düsseldorf, Germany
[c]Cluster of Excellence in Plant Sciences, Heinrich-Heine-Universität Düsseldorf, 40255 Düsseldorf, Germany
[d]Laboratory of Genetics, Wageningen University and Research, 6708 PB Wageningen, The Netherlands

ORCID IDs: 0000-0001-5012-2346 (G.W.v.E.); 0000-0002-7759-4869 (M.K.); 0000-0002-6816-586X (M.v.K.).

The complex nature of crop genomes has long prohibited the efficient isolation of agronomically relevant genes. However, recent advances in next-generation sequencing technologies provide new ways to accelerate fine-mapping and gene isolation in crops. We used RNA sequencing of allelic *six-rowed spike3* (*vrs3*) mutants with altered spikelet development for gene identification and functional analysis in barley (*Hordeum vulgare*). Variant calling in two allelic *vrs3* mutants revealed that *VRS3* encodes a putative histone Lys demethylase with a conserved zinc finger and Jumonji C and N domain. Sanger sequencing of this candidate gene in independent allelic *vrs3* mutants revealed a series of mutations in conserved domains, thus confirming our candidate as the *VRS3* gene and suggesting that the row type in barley is determined epigenetically. Global transcriptional profiling in developing shoot apical meristems of *vrs3* suggested that VRS3 acts as a transcriptional activator of the row-type genes *VRS1* (*Hv.HOMEOBOX1*) and *INTERMEDIUM-C* (*INT-C*; *Hv.TEOSINTE BRANCHED1*). Comparative transcriptome analysis of the row-type mutants *vrs3*, *vrs4* (*Hv.RAMOSA2*), and *int-c* confirmed that all three genes act as transcriptional activators of *VRS1* and quantitative variation in the expression levels of *VRS1* in these mutants correlated with differences in the number of developed lateral spikelets. The identification of genes and pathways affecting seed number in small grain cereals will enable to further unravel the transcriptional networks controlling this important yield component.

Identification of genomic variation is crucial for unraveling the relationship between genotype and phenotype and provides important insights into the genetic basis of agronomic traits in crop plants. Many crop species, including wheat (*Triticum aestivum*) and barley (*Hordeum vulgare*), are characterized by large genomes with regions of reduced recombination. The isolation of genes underlying important agronomic traits is therefore difficult and time consuming. However, next-generation sequencing (NGS) technologies and the generation of genomic reference sequences in these crops are providing new ways to accelerate the genetic analysis of traits. Whole-genome or targeted resequencing has been employed to aid in the fine mapping and identification of causal polymorphisms collectively termed as NGS-enabled genetics. Mapping by sequencing was first applied in the model species Arabidopsis (*Arabidopsis thaliana*; Schneeberger et al., 2009; James et al., 2013). This procedure is based on genome-wide resequencing of phenotypic bulks of mutant F2 individuals to fine-map the gene of interest. Mapping-by-sequencing based on whole-exome capture or RNA sequencing to reduce genome complexity has also been successfully applied for fine mapping in wheat and barley (Trick et al., 2012; Pankin et al., 2014; Liller et al., 2017). Although mapping by sequencing has proven successful to identify candidate genes, it still requires a substantial effort in generating and phenotyping large mapping populations. Furthermore, additional variation in the background may obscure the phenotypic effect of allelic variation at the target gene and mapping resolution may still be low in parts of the genome with low recombination.

An elegant method for gene identification without a segregating population is based on the analysis of multiple allelic mutants. Although the mutagenic treatment may affect many genes in a single genome, it is usually

[1] This research was funded by the German Cluster of Excellence on Plant Sciences (CEPLAS) EXC1028, the Priority Program (SPP1530, Flowering time control: from natural variation to crop improvement) and the Max Planck Society.

[2] These authors contributed equally to the article.

[3] Current address: Laboratory of Molecular Biology, Wageningen University and Research, 6708 PB Wageningen, The Netherlands.

[4] Address correspondence to korff@mpipz.mpg.de.

The author responsible for distribution of materials integral to the findings presented in this article in accordance with the policy described in the Instructions for Authors (www.plantphysiol.org) is: Maria von Korff (korff@mpipz.mpg.de).

A.W., G.W.v.E., M.K., and M.v.K. conceived and designed the experiments; A.W., G.W.v.E., and A.F. performed the experiments; A.W., G.W.v.E., A.P., and M.v.K. analyzed the data; A.W., G.W.v.E., and M.v.K. wrote the article.

[OPEN] Articles can be viewed without a subscription.

www.plantphysiol.org/cgi/doi/10.1104/pp.17.00108

only one gene or a very small set of genes that carry severe changes within all independent allelic mutants. Whole-genome sequencing of allelic mutants in Arabidopsis and rice (*Oryza sativa*) has successfully revealed candidate genes for the variant phenotype without any prior mapping (Nordström et al., 2013). To date, this approach has not been applied to the complex genomes of crops, presumably because of the lack of high-quality physical maps and the difficulty of distinguishing true allelic variants from homologous genes.

In barley, large collections of developmental and morphological mutants represent a valuable resource for gene identification and characterization (Druka et al., 2011). These have been generated by physical and chemical mutagenesis since the early 20th century to explore the potential of mutation breeding in crop improvement (Ahloowalia et al., 2004; Lundqvist, 2014). Primary mutants were induced or discovered in different cultivars, which after mutagenesis contained a different spectrum of background mutations. Therefore, many mutant loci were introgressed into the common genetic background Bowman by repeated back-crossing and phenotypic selection (Druka et al., 2011). This resulted in a large collection of introgression lines (ILs) in the cultivar (cv) Bowman with a relatively small genetic interval originating from the donor that contains the mutated locus. In addition, many of these mutant phenotypes were intercrossed to identify allelic mutant series for different morphological, developmental, and physiological traits. The collection has proven particularly valuable for studying the genetic control of plant and spike architecture (Druka et al., 2011; Koppolu et al., 2013; Liller et al., 2015).

In cereals, plant and spike architecture influence the number of seeds, one of the most important yield component traits. The spike of barley forms a triple spikelet meristem with one central spikelet meristem and two lateral spike meristems. The seeds on the barley spike can be arranged either in two or six rows. In the two-rowed spike, only the central spikelet is fertile, while in the six-rowed spike, all three spikelets give rise to seeds. The genes underlying the *six-rowed spike* (*vrs*) loci *vrs1* and *vrs4* have been identified as key inhibitors of lateral spikelet development, and their loss of function leads to the development of six-rowed spikes. *VRS1* encodes a HD-ZIP transcription factor (Hv.Hox1; Komatsuda et al., 2007). *VRS4* encodes a LATERAL ORGAN BOUNDARY transcription factor that is homologs to the maize (*Zea mays*) *RAMOSA2* (*RA2*) and acts upstream of *VRS1* (Koppolu et al., 2013). In addition, a number of row-type mutants display an *intermedium spike* (*int*) phenotype with varying two- or six-rowed patterns. These intermedium (*int/vrs*) mutants show enlarged lateral florets which may or may not develop into kernels, depending on the position on the spike and the environment (Lundqvist and Lundqvist, 1987, 1988b).

More than 130 intermedium mutants have been isolated, of which 60 were shown to be mutated in one of nine genes (Gustafsson and Lundqvist, 1980). The most frequent intermedium mutant is *int-c*, which has been identified as a barley homolog of *TEOSINTE-BRANCHED1* (Ramsay et al., 2011), a TCP transcription factor and major domestication related gene affecting shoot branching in maize (Studer et al., 2011; Studer and Doebley, 2011). Double mutants of different *int* loci lead to typical six-rowed plants, suggesting that *int* genes and *VRS1* might interact in the same pathway (Lundqvist et al., 1988a, 1988b; Lundqvist and Lundqvist, 1988a). In a comprehensive analysis, we have classified 36 different row-type mutants based on their shoot and spike architecture (Liller et al., 2015). Allelic *vrs3/int-a*, *int-c*, *vrs1*, and *vrs4* mutants and derived introgression lines showed comparable macroscopic phenotypes, such an increase in the number of seeds per spike and a reduction in tiller number at maturity compared to their two-rowed wild-type parents. Taken together, phenotypic studies have shown that *int-a*, *int-c*, *vrs1*, and *vrs4* are genetically separate loci, which likely interact to control lateral spikelet development in barley. These row-type mutants now provide a valuable resource to identify the underlying mutations and investigate the molecular network controlling spikelet development and fertility. The causative genes and mutations for *vrs1*, *vrs4*, and *int-c* are known, while the gene underlying the *vrs3* locus has so far not been identified.

We performed RNA sequencing of developing spike meristems in the allelic *vrs3.f/int-a.1* mutants, and in addition in *vrs1*, *vrs4.k*, and *int-c*, all introgressed into cv Bowman (Druka et al., 2011). We demonstrate that RNA sequencing of allelic and epistatic mutants provides a powerful method for simultaneous gene isolation and functional analysis in barley.

RESULTS

Variant Calling on RNA Sequencing Reads Reveals a Candidate Gene for the *vrs3/int-a* Mutation

Our first aim was to determine the size and location of the introgressions in the two independent ILs carrying the allelic *vrs3.f* and *int-a.1* mutations (Lundqvist et al., 1988a). Both mutants exhibit fertile lateral spikelets resulting in an increased number per spike when compared to cv Bowman (Fig. 1; Supplemental Fig. S1), corroborating previous reports (Lundqvist and Lundqvist, 1988b; Koppolu et al., 2013; Liller et al., 2015). The development of additional lateral spikelets, which mainly occurred at the middle part of the spike, was not associated with a significant change in rachis internode number (Supplemental Fig. S1, A and B).

We hypothesized that the causal gene is likely located within the introgressed regions common to both ILs. In addition, our objective was to identify the gene variants underlying the row-type phenotype (Fig. 1) in both allelic mutants. To accomplish this, we sequenced total RNA extracted from the main shoot apex (MSA) when the lemma and stamen primordium started to develop (Waddington stages W3.0–W3.5). At this stage, the first floral organ primordia differentiate and the stem

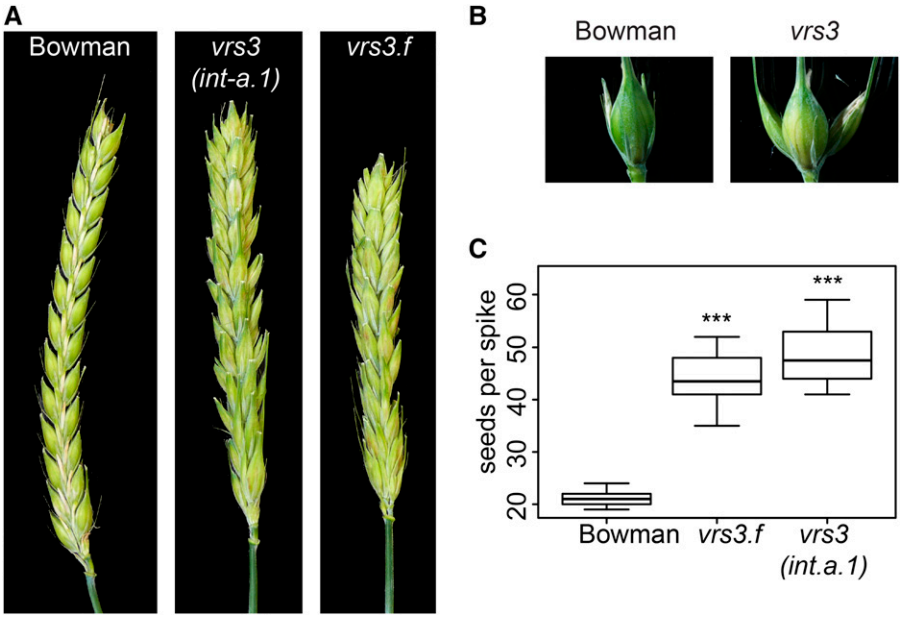

Figure 1. Spike phenotype of *vrs3* plants. A, The intermedium row-type phenotype of *vrs3*, which exhibits fertile lateral spikelets at the upper part of the spike. The awns were removed from the spike to visualize the difference between the mutant and wild type. B, In cv Bowman, only the central spikelet is developed; in the upper part of *vrs3* the central and lateral spikelets give rise to seeds. C, *vrs3*(*int-a*) and *vrs3.f* mutants have a significantly increased seed number per spike when compared to the wild type. Significant differences were determined with a one-way ANOVA, $P \leq 0.01$, $n = 10$ spikes.

elongation is initiated. Moreover, initial differences between six-rowed *vrs* mutants and wild type are clearly visible (Koppolu et al., 2013). RNA sequencing was carried out in the ILs, the backcross recipient cv Bowman and cv Bonus, the parental line of *int-a.1*. Hakata2, the original parent of *vrs3.f*, was not available for sequencing. Reads obtained from RNA sequencing of the MSA tissue were mapped to a combined set of high confidence (HC) and low confidence (LC) predicted coding sequences of cv Morex (International Barley Genome Sequencing Consortium, 2012). The reads were mapped to the barley reference using Burrows Wheeler Aligner (BWA)-MEM (Langmead and Salzberg, 2012; Li, 2013) resulting in a mapping rate of 80%.

Mapping quality filtered reads obtained from BWA-MEM alignments were subjected to variant calling. After stringent filtering of putatively false positive single nucleotide polymorphisms (SNPs), resulting variants of each mutant line were compared to variants obtained from cv Bowman. This comparison resulted in alleles specific to each mutant line and thus revealed the size, number, and position of the introgressions in the ILs. The mutant line *vrs3.f* contained three introgressions on chromosome 1H, 2H, and 4H, while the *int-a.1* mutant carried four introgressions on chromosome 1H, 6H, and 7H (Fig. 2). We detected an overlap between the introgressions in *vrs3.f* and *int-a.1* located on chromosome 1H in the interval of 35.69 cM to 52.55 cM. The region comprises 2075 HC and LC genes. This target interval is useful to delimit the number and position of possible candidate genes. However, the chromosomal position of genes may not be correct. We therefore considered all genetic differences between the ILs and the parental lines regardless of their genomic position. Polymorphisms shared between any of the two ILs and Morex were excluded as candidates for the *vrs3*/*int-a* phenotype. Furthermore, variants obtained from the *int-a.1* mutant were compared to the *int-a.1* parental line cv Bonus. Only seven genes carried unique nonsynonymous mutations that differentiated *int-a.1* from cv Bonus, cv Bowman, and cv Morex (Table I; Supplemental File S1). Mutations differentiating *vrs3.f* from cv Bowman and cv Morex were detected in 196 genes. From those genes only one gene, MLOC_69611.1, carried a unique mutation in *int-a.1* and *vrs3.f* (Table I). Both MLOC_69611.1 alleles in the mutant lines carry deletions causing frame shifts (AT > A at position 394 in *vrs3.f*, TGC > T at position 1667 in *int-a.1*). Analysis of the conserved domains of MLOC_69611.1 showed that the gene is a putative histone demethylase containing a zinc-finger as well as a Jumonji (Jmj) C and N domain. The *vrs3.f* mutant contains a deletion of one nucleotide changing the amino acid sequence anterior to the zinc finger domain. *Int-a.1* contains a deletion of two base pairs prior to the JmjN domain of this protein, resulting in a frame shift. Taken together, our variant calling revealed that MLOC_69611.1 carries unique mutations in *vrs3.f* and *int-a.1* resulting in a nonfunctional protein. Therefore, we selected MLOC_69611.1 located on chromosome 1H at 47.52 cM as a prime candidate for the *vrs3* locus.

Several additional allelic variants of *vrs3* are available, most of them originate from x-ray or neutron-induced mutagenesis screens. The candidate gene MLOC_69611.1 was resequenced in 19 independent *vrs3* mutants, obtained from the Nordic Genome Resource Center (http://www.nordgen.org). The candidate gene MLOC_69611.1 contained an indel, causing a frame shift in five genotypes, six genotypes carried a premature stop codon, six genotypes contained a nonsynonymous SNP in or close to conserved domains, and two genotypes carried a nonsynonymous SNP

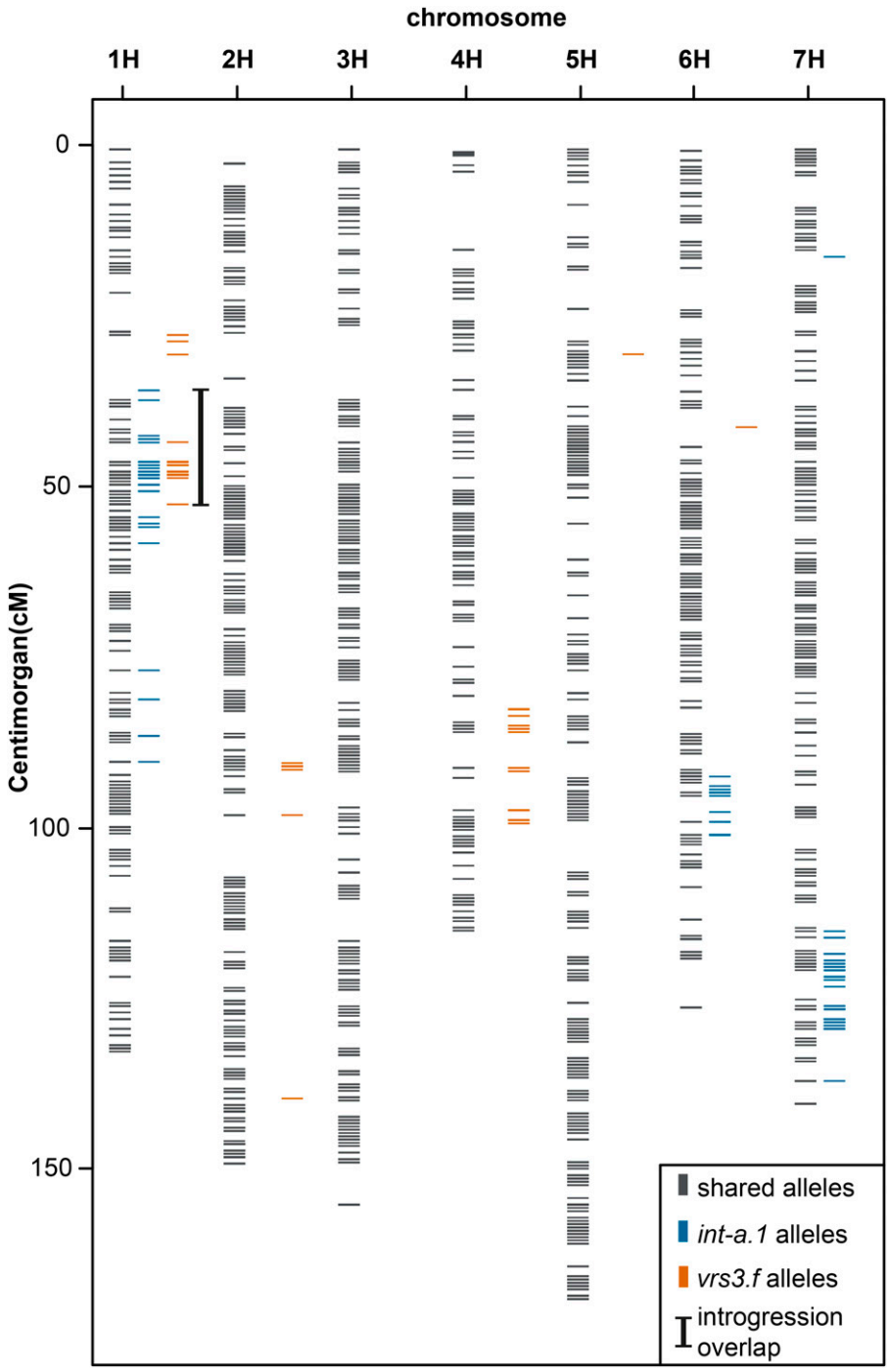

Figure 2. Variant calling in *vrs3.f* and *int-a.1*. Genes carrying mutations in *vrs3.f* and *int-a.1* were identified and placed on the barley POPSEQ map. Introgression regions are detected by variant calling between the respective mutant line and cv Bowman. The overlapping introgression region of *vrs3.f* and *int-a.1* is indicated with a black bar.

close to an intron-exon junction (Fig. 3; Supplemental Table S1). This confirmed that MLOC_69611.1 is indeed the gene underlying the *vrs3* mutant phenotype. Phylogenetic analysis indicated that the MLOC_69611.1 protein shows the highest similarity to the evolutionary conserved JMJD2 group II of JmjC domain-containing proteins (Supplemental Fig. S3). The closest orthologs of MLOC_69611.1 are the Lys-specific demethylases JMJ13 (At5g46910) in Arabidopsis and JMJ706 (Os10g42690) in rice (Supplemental Table S2). Furthermore, comparison of the JmjC domains revealed a 95.97% identity between VRS3 and Os.JMJ706 and an 83.87% identity between VRS3 and At.JMJ13 (Supplemental Table S2). Os.JMJ706 is mainly involved in the removal of a methyl group from the Lys 9 of the histone H3 protein (H3K9me), whereas At.JMJ13 has an H3K27me3 demethylase activity (Sun and Zhou, 2008; Crevillèn et al., 2014).

Table I. *Introgression overview of vrs3.f and int-a.1 mutants*

	vrs3.f		*vrs3(int-a.1)*		*vrs3.f/vrs3(int-a.1)* Overlap	
Introgression intervals	Chromosome	Position (cM)	Chromosome	Position (cM)	Chromosome	Position (cM)
	1H	27.4 to 52.5	1H	35.7 to 58.2	1H	35.7 to 52.6
	2H	90.4 to 97.8	1H	78.8 to 90.2		
	4H	82.7 to 99.2	6H	92.3 to 101.0		
			7H	115.4 to 137.3		
No. of genes in introgression	2639		4046		2075	
Unique nonsynonymous mutations in the ILs	196		7		1 (MLOC_69611.1)	

Comparative Transcriptional Profiling of *vrs3 vrs1, vrs4,* and *int-c* Mutants

Comparative phenotyping of spike architecture in *vrs1*, *vrs3(int-a.1)*, *vrs4.k*, and *int-c.5* revealed that these mutants showed quantitative differences in spikelet development. In *vrs1* and *vrs4.k* plants, the spike was fully six-rowed, whereas in the *vrs3* and *int-c.5* mutants the lower third and upper parts of the spike were two-rowed and the middle of the spike appeared six-rowed (Supplemental Fig. S1). Moreover, both *vrs3* and *vrs4.k* formed additional lateral spikelets, whereas *vrs1* and *int-c.5* did not. To explore the molecular basis of quantitative variation in spikelet development, we performed parallel transcriptional profiling of *vrs1*, *vrs3*, *vrs4.k*, and *int-c.5* mutants in the Bowman background (Supplemental Fig. S2) at W3.5 and W5.0. At the stamen primordium stage (W3.5), the first floral organ primordia start to differentiate. The induction of floret primordia on the inflorescence continues until the awn primordium stage (W5.0). The mutations in *vrs3(int-a.1)* and *int-c.5* are both characterized by a small deletion causing a frame shift in a histone demethylase and an ortholog of *teosinte branched1* (*TB1*), respectively. The *vrs4.k* mutant carries a small deletion causing a nonsense mutation in *Ra2*; and the *vrs1* mutant contains a nonsynonymous SNP in a homeobox (HOX) transcription factor (Komatsuda et al., 2007; Ramsay et al., 2011; Koppolu et al., 2013). We identified transcripts of 30,174 genes at W3.5 and W5.0 (Supplemental Table S3). When compared to cv Bowman, 146 differentially regulated transcripts (DRTs) were identified in *vrs1*, 414 in *vrs4.k*, 524 in *vrs3(int-a.1)*, and 87 in *int-c.5* (Fig. 4A; Supplemental Fig. S4). From the 524 DRTs affected in *vrs3(int-a.1)*, 426 were down-regulated, while only 98 were significantly up-regulated (Supplemental Fig. S4). The high number of repressed versus induced DRTs suggests that VRS3 acts primarily as a transcriptional activator.

To assess whether any of the DRTs identified in *vrs3(int-a.1)* were also affected in *vrs1*, *vrs4.k*, or *int-c.5* and vice versa, a hierarchical cluster analysis (Eisen et al., 1998) was performed. Hierarchical clustering of mutants based on all DRTs grouped *vrs1*, *vrs3(int-a.1)*, and *vrs4.k* together, while *int-c* clustered separately (Fig. 4B). This indicated a high overlap in DRTs among *vrs1*, *vrs3(int-a.1)*, and *vrs4.k*, while expression variation in *int-c* differed from the former. More than 50% of the genes differentially regulated in *vrs1* were also affected in *vrs4.k* and *vrs3(int-a.1)* (Fig. 4A). Among the repressed DRTs in *vrs1*, *vrs4.k*, and *vrs3(int-a.1)*, we detected several His kinases involved in cytokinin and abscisic acid signaling (Supplemental Tables S4 and S5). In addition, PIF helicases, involved in maintenance of genome stability were repressed in the *vrs3(int-a.1)*, *vrs1*, and *vrs4.k*. Furthermore, an ortholog of the Jumonji N/C and zinc finger domain-containing protein: *RELATIVE OF EARLY FLOWERING6* (*REF6*; MLOC_50345.1) was down-regulated in all three mutant genotypes. In Arabidopsis, REF6 acts as a positive regulator of flowering in a FLC-dependent pathway and may play a role in brassinosteroid signaling (Noh et al., 2004; Yu et al., 2008).

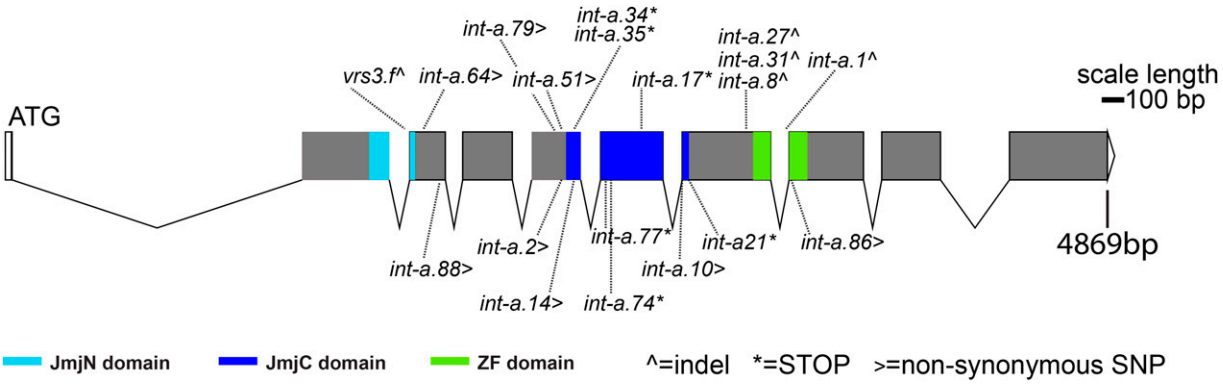

Figure 3. VRS3 is a putative histone demethylase with a Jumonji domain. Gray bars indicate the exons, and the conserved JmjN and JmjC domains are indicated in light blue and dark blue, respectively. The zinc finger (ZF) domain is indicated in green.

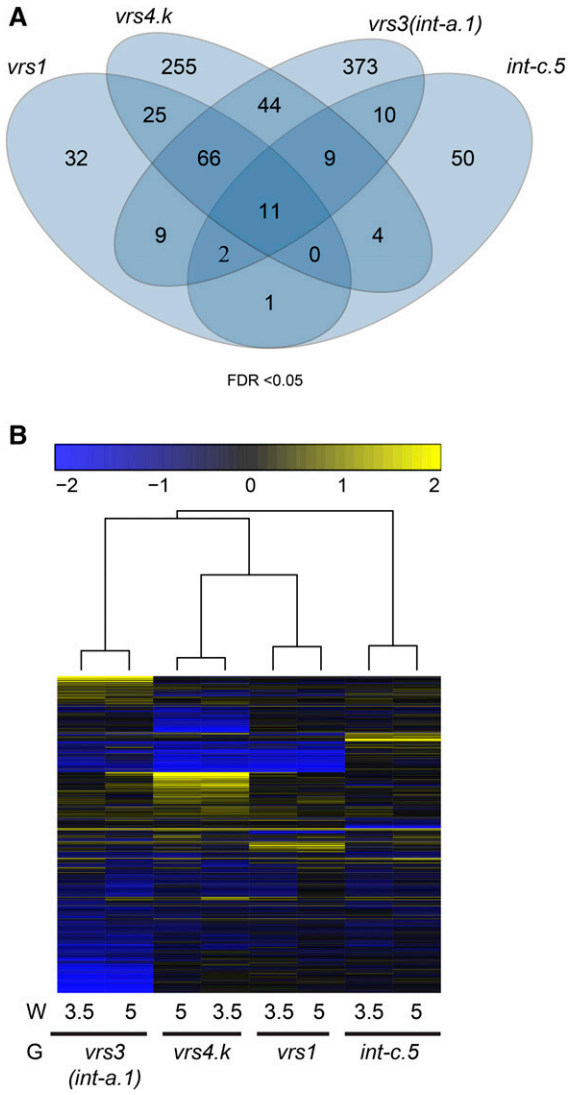

Figure 4. Transcriptional profiling of row-type mutants. A, Venn diagram showing the overlap in differentially regulated genes (FDR 5%) among *vrs1*, *vrs3(int-a)*, *vrs4.k*, and *int-c.5*. B, Hierarchical cluster analysis of all DRTs showing the expression at Waddington stages W3.5 and W5.0 for all four genotypes (G).

Interestingly, *VRS1* (AB259783.1) was down-regulated in *vrs3(int-a.1)*, *vrs4.k*, and *int-c.5*, suggesting that all three genes act as positive regulators of *VRS1* expression in barley. When compared to *VRS1*, which is specifically expressed in the developing inflorescence, *VRS3* shows a more broad expression profile throughout different tissues (Supplemental Fig. S5). RNA sequencing also showed a down-regulation of another HOX-like transcription factor (MLOC_77488.1; hereafter referred to as HOX2) in *vrs3(int-a.1)*, *vrs4.k*, and *int-c.5* (Supplemental Table S4). Taken together, the transcriptional profiling of *vrs3* MSA revealed a high number of down-regulated genes, suggesting that VRS3 is a transcriptional activator. In addition, parallel expression profiling of different row-type mutants revealed that a large subset of DRTs was shared between *vrs1*, *vrs3*, and *vrs4*. Finally, *vrs3*, *vrs4*, and *int-c* were all characterized by a quantitative down-regulation of *VRS1*.

VRS1 and *INT-C* Transcripts Are Reduced in *vrs3*

RNA sequencing revealed that the transcript levels of *VRS1* were lower in *vrs3* mutant plants. To further explore the effect of VRS3 on *VRS1*, *INT-C*, and *VRS4* expression, we performed quantitative real-time PCR (qRT-PCR) at different developmental stages from the initiation of spikelet primordia (W2.0) until early stages of pistil development (W6.0). In wild-type Bowman plants, the expression levels of *VRS1*, *VRS4*, and *INT-C* were upregulated during development to a much higher extent in the wild type compared to the *vrs3* mutant plants (Fig. 5, A–D). This suggested that VRS3 promoted the induction of *VRS1*, *VRS4*, and *INT-C*. RNA sequencing further demonstrated that the transcript levels of *VRS1* were lower in *vrs4* and *int-c* mutant plants. We, therefore, compared the effects of VRS3, VRS4, and INT-C on the expression of *VRS1* using qRT-PCR at the stamen and carpel primordium stages. Expression of *VRS1* was reduced in *vrs3*, *vrs4*, and *int-c* mutants compared to cv Bowman in both stages (Fig. 5E). However, *VRS1* expression levels differed between mutants, the *VRS1* transcript levels were lowest in the *vrs4.k* mutant, followed by *int-c.5*, *vrs3 (int-a.1)*, and *vrs3. f. VRS1* expression was also reduced in *vrs3* (*int-a.1)* and *vrs3* (*int-a.64)*, both in the background of cv Bonus and *vrs3 (int-a.8)* in the background of cv Foma. Consequently, we showed that all three genes, *VRS3*, *VRS4*, and *INT-C*, are positive regulators of *VRS1* expression. Interestingly, *INT-C* expression was, like *VRS1*, reduced in both *vrs4* and *vrs3*, suggesting that these genes also act on *INT-C* expression (Fig. 5F).

When *VRS4* expression was analyzed in the different *vrs* and *int-c* mutants at W3.5 and W5.0, a significant reduction of VRS4 expression was only observed in *vrs4.k* in the Bowman background (Supplemental Fig. S6A). This indicates that the effect of *vrs3* on *VRS4* expression were not consistent across stages and genetic backgrounds. Furthermore, a small but significant increase in *VRS3* expression levels was observed in the *vrs4.k* mutant (Supplemental Fig. S6B).

VRS1 is known to determine the row type and its effect is modified by INT-C (Ramsay et al., 2011). We therefore concluded that the quantitative down-regulation of *VRS1* and *INT-C* might be linked to the intermediate row-type phenotype in *vrs3* mutants (Fig. 6).

DISCUSSION

Whole-genome sequencing of allelic variants has been employed to identify candidate genes without prior mapping in model systems such as Arabidopsis and rice with relatively small genomes (Nordström et al., 2013). Because of the genome size of barley, sequencing whole genomes in multiple mutants is not

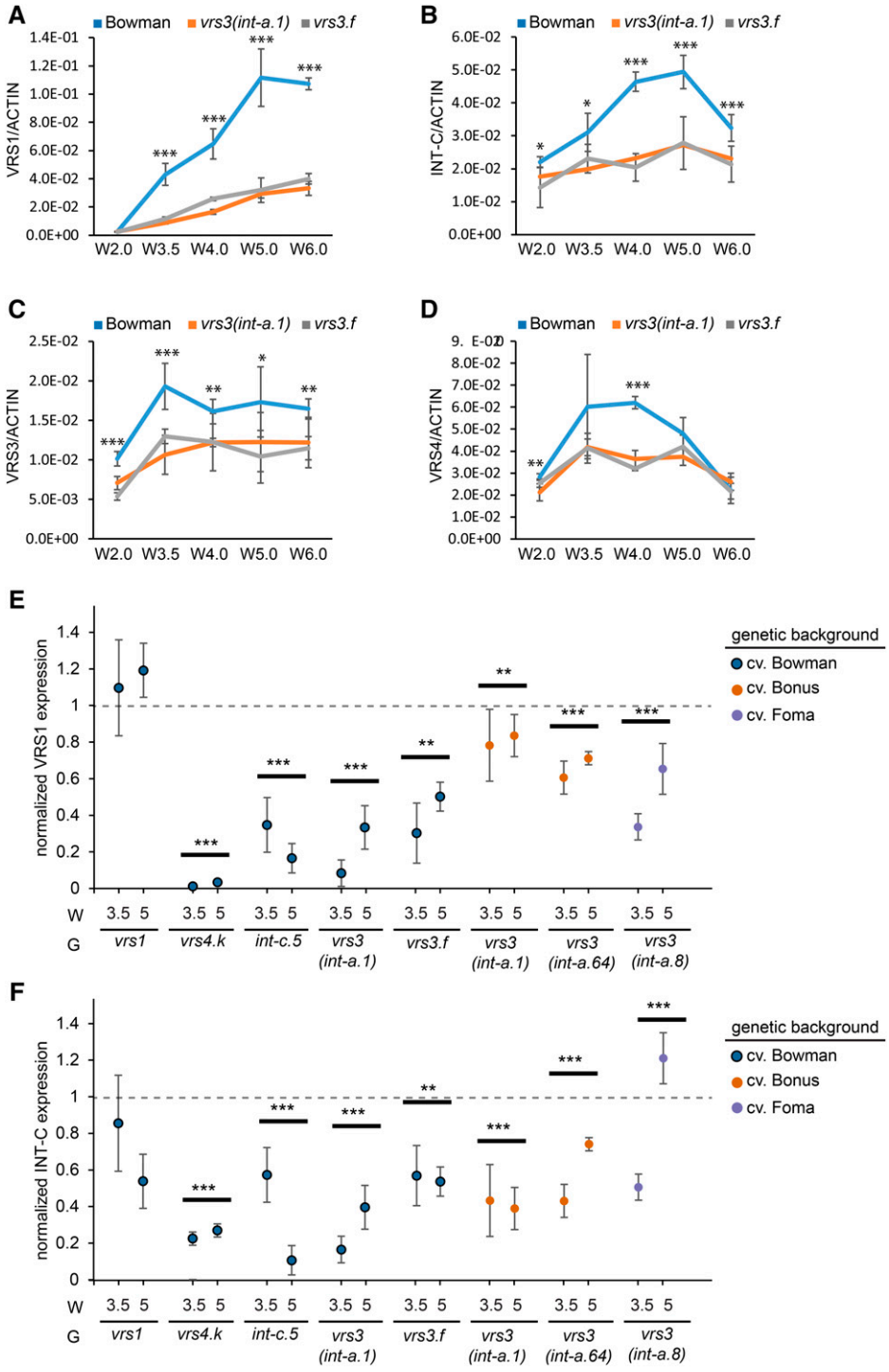

Figure 5. Expression of *VRS1*, *VRS3*, *VRS4*, and *INT-C* in wild type and *vrs3* mutant genotypes. A to D, Expression of *VRS1* (A), *INT-C* (B), *VRS3* (C), and *VRS4* (D) throughout inflorescence development determined with qRT-PCR. Error bars ± SD, $n \geq 3$ replicates. Significant differences per time point are based on a Student's *t* test (Bowman versus *vrs3(int-a.1)* and *vrs3.f* ILs). E and F, Expression of *VRS1* (E) and *INT-C* (F) in various mutant backgrounds (G) at Waddington stages W3.5 and W5.0 determined with qRT-PCR. All expression values were compared to their respective wild-type backgrounds. The gray dashed line represents the corrected value for the wild-type control. Blue dots represent expression in *vrs1*, *vrs4.k*, *int-c.5*, *vrs3(int-a.1)*, and *vrs3.f* ILs in cv Bowman. Orange dots represent expression in *vrs3(int-a.1)* and *vrs3(int-a.64)* in cv Bonus. Purple dots represent *vrs3(int-a.8)* in cv Foma. Significant differences in expression of *VRS1* or *INT-C* in the different mutants compared to the respective wild type across stages was determined using an two-factorial ANOVA with genotype (Bowman versus *vrs3(int-a.1)* and *vrs3.f* ILs) and stage as factors, followed by a post hoc Dunnett's test for multiple comparisons ($n \geq 3$ biological replicates). Asterisks indicate significant differences: $*P \leq 0.1$, $**P \leq 0.05$, $***P \leq 0.01$.

practical due to the cost and the difficulty of interpreting the large datasets. Recently, a method was presented for gene isolation in allelic barley mutants based on flow sorting and sequencing of a single chromosome that carried a known gene for the *eciferum* mutation (Sánchez-Martín et al., 2016). In addition, two stem rust resistance genes, *Sr22* and *Sr45a*, were isolated in wheat using independent ethyl methane sulfonate induced suppressor lines and sequencing of libraries enriched for nucleotide binding and Leu-rich repeats (Steuernagel et al., 2016). These methods enabled the identification of induced mutations without the need for positional fine mapping but still required prior knowledge of the chromosome position (Sánchez-Martín et al., 2016) or of the type of gene affected (Steuernagel et al., 2016). In addition, these methods are technologically and

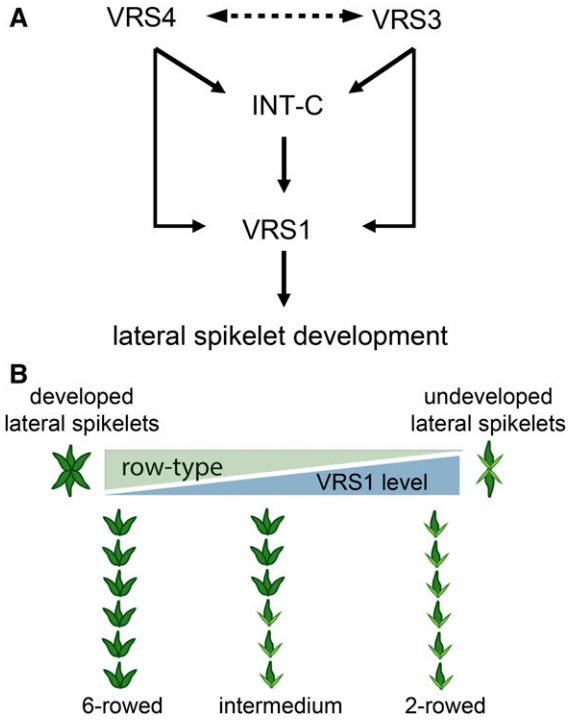

Figure 6. VRS1 expression levels affect lateral spikelet development. A, *VRS1* is significantly down-regulated in all row-type mutants. Similarly, *INT-C* is significantly down-regulated in *vrs3* and *vrs4*, indicating that the latter two act on *INT-C* expression. B, Top-down view on the triple spikelet. *VRS1* expression levels determine lateral spikelet development; in the absence of *VRS1* (*vrs1* or *vrs4* mutants) the spike is fully six-rowed. Intermedium mutants such as *vrs3* and *int-c.5* with partially developed spikelets exhibit reduced expression levels of *VRS1* when compared to the two-rowed wild type, which does not develop lateral spikelets.

computationally demanding. We instead applied RNA sequencing as a cost-efficient and simple method for gene identification without the need for mapping. The availability of allelic introgression lines enabled us to significantly reduce the target interval and thereby reduced the number of possible candidate genes. However, for the identification of the causal gene and sequence variants, we considered all polymorphic genes regardless of their genomic position. This is important when the reference sequence contains errors. It also demonstrates that our method does not rely on the availability of introgression lines or any prior mapping information. The identification of the causative mutation, however, was only possible because the target gene was expressed in the sequenced tissue and the mutation was located in the transcribed part of the gene.

Through RNA and Sanger sequencing of allelic *vrs3* mutants, we were able to identify the candidate gene underlying *vrs3* as a putative histone Lys demethylase with a conserved zinc finger and Jumonji C and N domain. Methylation on the histone H3 Lys 4 and Lys 36 (H3K4 and H3K36, respectively) is often associated with actively transcribed genes, while methylation of H3K9, H3K27, and H4K20 is associated with repressed genes (Kooistra and Helin, 2012). Thus, removal of such methylation by JmjC domain-containing proteins can lead to both transcriptional silencing and activation, respectively. The targets of histone Lys demethylases are genes with diverse functions, which is likely the reason for various developmental phenotypes in JmjC-domain protein mutants. For example, the JmjC domain-containing proteins EARLY FLOWERING6 and REF6, are involved in flowering time control in Arabidopsis (Noh et al., 2004). Moreover, JmjC-mediated histone demethylation at the *FLC* locus at elevated temperature is known to prevent premature early flowering (Gan et al., 2014). In rice, the JMJ703, a histone H3 Lys 4 (H3K4) demethylase, is required for stem elongation and transposon silencing (Chen et al., 2013; Cui et al., 2013). The barley *VRS3* is similar to the JMJD2 group II of Lys demethylases and exhibits a high similarity to the rice JMJ706, which encodes for a histone H3 Lys 9 di- and tri- (H3K9me2 and H3K9me3) demethylase (Sun and Zhou, 2008). The H3K9me2 and me3 are repressive modifications in heterochromatin and euchromatin contexts, respectively, (Liu et al., 2010), suggesting that JMJ706 is necessary for the activation of specific genes (Sun and Zhou, 2008). This scenario may hold true also for VRS3, as suggested by our expression analysis of *vrs3(int-a.1)*. Here, the group of down-regulated DRTs was about 4-fold higher when compared to the up-regulated DRTs. In the context of a putative VRS3 function, the "down-regulation" should be interpreted as absence of activation and "up-regulation" as lack of silencing in the mutant. This hypothesis was further supported by analysis of VRS1 and INT-C expression over development. The induction of both genes was strongly enhanced in the wild type compared to the *vrs3* mutant plants. Thus, we suggest that VRS3 acts as a positive regulator of gene expression, possibly by erasing the repressive methylation at histones of its target genes. How many of the genes identified as misregulated by RNA sequencing are direct targets of VRS3 is currently unknown, but INT-C and VRS1 are the prime candidates, as they showed low transcript amounts in multiple *vrs3* alleles, when compared to wild type and their mutants show similar floral phenotypes. This again leads to functional analogy with rice JMJ706, which regulates floral organ development (Sun and Zhou, 2008). In barley, loss of *VRS3* function results also in an alteration in floral organ number (Lundqvist and Lundqvist, 1988b). JMJ706 affects the histone methylation on the *degenerated hell1* locus, which encodes a putative lateral organ boundaries domain transcription factor (Sun and Zhou, 2008). In our analysis, the LOB-domain transcription factor VRS4 was not consistently down-regulated in the *vrs3* mutants. Vice versa, the *VRS3* expression was not strongly affected in the *vrs4* mutant. Previous studies have demonstrated that in *vrs4* mutants, *VRS1* is significantly down-regulated, placing *VRS4* upstream of *VRS1* (Komatsuda et al., 2007; Sakuma et al., 2013). Whereas expression of *VRS1* was not detected in the

vrs4 mutant, RNA sequencing and qRT-PCR analysis showed that *VRS1* was expressed in *vrs3* but at lower levels compared to Bowman. This could be due to only partial removal of the repressive modification(s) and subsequently weaker transcriptional change as observed for several histone demethylase mutants in Arabidopsis (Yu et al., 2008; Miura et al., 2009; Searle et al., 2010).

VRS1 expression levels in *vrs3*, *vrs4*, and *int-c* mutant genotypes suggested that variation in the development of lateral spikelet between the six-row mutants *vrs1* and *vrs4* and the intermedium mutants *vrs3* and *int-c* was mediated by quantitative variation in *VRS1* expression. No expression of *VRS1* in *vrs4* or nonfunctional *vrs1* alleles resulted in a fully six-row spike, while partial induction of *VRS1* in *vrs3* and *int-c* correlated with an intermedium spike phenotype and partial development of lateral spikelets.

Interestingly, *INT-C* expression was also significantly lower in the *vrs3* mutant. In maize, the HOX transcription factor GRASSY TILLERS1 (GT1) is downstream of TB1 and involved in the shade avoidance pathways (Whipple et al., 2011). GT1 functions mainly during vegetative growth, while VRS1 functions in inflorescence development. However, both have a similar developmental role in preventing the outgrowth of lateral buds/meristem. Therefore, we propose that, in analogy with the maize TB1 and GT1, VRS1 is downstream of INT-C in regulating lateral spikelet development. It remains to be elucidated if VRS3 affect *VRS1* directly or through the transcriptional control of *INT-C*.

CONCLUSION

We presented a fast and efficient method for gene identification with no requirement for recombination or the analysis of mapping populations. This is important when analyzing the large genomes of barley and wheat, which are characterized by extensive regions of suppressed recombination. We identified the gene underlying *vrs3* as a putative histone demethylase with a jumonji domain. Our transcriptional profiling suggested that VRS3 is a regulator of *VRS1* and *INT-C* expression, which controls lateral spikelet development. The *vrs3* locus is well known for its increased seed number per spike, an important yield component in small grain cereals. Unraveling the genetic basis of agronomic traits in crop plants is necessary to further improve crop yield.

MATERIALS AND METHODS

Plant Growth Conditions and Phenotyping

Plants were sown in 96-cell growing trays using "Mini Tray" (Einheitserde) as soil. To equalize germination, the trays were kept in the dark at 4°C for 3 days, after which the seedlings were grown under long-day conditions (16 h, 22°C day; 8 h, 18°C night). The developmental stage of the MSA of *vrs3.f*, *int-a*, *vrs1*, and *vrs4* was determined according to the quantitative scale of Waddington et al. (1983). The quantitative scale by Waddington et al. (1983) is based on the progression of the most advanced floret primordium and carpel of the inflorescence. At the double-ridge stage (W1.5–2.0), the first spikelet primordia on the shoot apex emerge; this specifies a reproductive MSA. The first lemma primordium start to develop at W3.0; at this stage the first differences between two-rowed and six-rowed *vrs* mutants start to occur (Koppolu et al., 2013). The stem elongation and differentiation of the first floral organ primordia occurs at the stamen primordium stage (W3.5). The induction of floral organ primordia continues until the awn primordium stage, which is marked by W5.0.

Plant Material

For the RNA sequencing of the mutants, near-isogenic lines in Bowman background were used. All mutants and parental lines were obtained from the U.S. Department of Agriculture (https://npgsweb.ars-grin.gov/) or from the Nordic Gene Bank (http://www.nordgen.org/). For *VRS3*, two mutants were sequenced: *vrs3.f* (GSHO 2056) and *int-a.1* (GSHO 2055), both backcrossed into the cultivar (cv) Bowman. The *vrs3.f* mutant originates from a gamma-ray-induced mutant in Hakata 2, and the *vrs3(int-a.1)* mutant from an x-ray-induced mutant in cv Bonus. For comparison of *vrs3* with other row-type genes using RNA sequencing, *vrs1*, *vrs4*, and *int-c* mutants were used. The *vrs1* mutant (GSHO 1907), which is a naturally occurring variant in most six-rowed barleys (Druka et al., 2011), has a C 1020 G, resulting in a nonsynonymous F075L change. The gamma-ray-induced *vrs4.k* mutant (GSHO 1986) has a C 072 deletion, resulting in a nonsense mutation. The x-ray-induced *int-c.5* mutant (GSHO 2003) carries a C 882 deletion causing a frame shift. These lines were also used for qRT-PCR confirmation. In addition, the *vrs3* mutants *int-a.1* (NGB115419), *int-a.64* (NGB115482), and *int-a.8* (NGB115426) were used to verify down-regulation of *VRS1* and *INT-C* using qRT-PCR. The *int-a.64* originates from an isopropyl methanesulfonate mutagenesis in cv Bonus, and *int-a.8* is an x-ray-induced mutant in cv Foma. The stock numbers and mutagenic agents of the 19 different allelic *vrs3* lines used to verify the selected candidate gene are listed in Supplemental Table S1.

RNA Isolation and Sample Preparation for RNA Sequencing

RNA was isolated from tissue of the MSA harvested from plants grown under long day conditions (16 h, 22°C day; 8 h, 18°C night). MSA tissue was harvested at W3.0 to W3.5 for *vrs3.f* and *vrs3*(*int-a.1*). For *vrs1*, *vrs4.k*, *vrs3*(*int-a.1*), and *int-c.5*, apex tissue was isolated at W3.5 and W5.0. The samples were harvested at the middle of the day, 6 to 8 h before the end of the light period. Before sampling, the developmental stage of the MSA was verified by dissecting three plants per genotype. For sampling the apex, leaves surrounding the MSA were removed manually, and the apex was cut using a microsurgical stab knife (5-mm blade at 15° [SSC#72-1551]). Samples were collected in three individual biological replicates. For each biological replicate, at least 10 MSA were pooled. All MSA harvested for RNA extraction were frozen immediately in liquid nitrogen and stored at −80°C. For RNA isolation, the pooled MSA were ground, dissolved in 500 μL TRIzol reagent (Invitrogen), and incubated for 5 min at room temperature. Next, 100 μL of chloroform was added, and the sample was homogenized, incubated for 2 min, and centrifuged for 15 min at 4°C. After phase separation, isopropanol was added to the aqueous phase, which was subsequently incubated for 10 min at room temperature and further purified using an RNA easy Micro Kit (Qiagen). Before RNA sequencing, the residual DNA was removed using a DNA-free kit (Ambion), and the quality of the RNA was tested using a bio analyzer (Agilent). The Illumina cDNA libraries were prepared according to the TruSeq RNA sample preparation (version 2; Illumina). A cBot (Illumina) was used for clonal sequence amplification and generation of sequence clusters. Single-end sequencing was performed using a HiSeq 2500 (Illumina) platform by multiplexing eight libraries, resulting in ~18 million reads per library. The initial quality control of the raw reads was performed using the FastQC software (version 0.10.1; https://www.bioinformatics.babraham.ac.uk/projects/fastqc/). The adaptors and short reads were trimmed using the Trimmomatic platform and embedded within the trinity pipeline (Grabherr et al., 2011; https://github.com/trinityrnaseq/trinityrnaseq/wiki) using the following default criteria: phred 33, leading and trailing 3, sliding window 4:15, and a minimum read length of 36.

Variant Calling of the RNA Sequencing Reads

The obtained RNA sequencing reads were mapped to a combined set of HC and LC predicted coding sequences of barley (*Hordeum vulgare*) cv Morex (IBGC, 2012) with BWA-MEM (version 0.7.15; Li, 2013). To ensure a high mapping rate even if distantly related barley cultivars are used, a mismatch penalty of 3 was used. PicardTools (version 1.1.00; http://broadinstitute.github.io/picard/) CollectAlignmentSummaryMetrics was applied on resulting SAM files for

evaluation of mappings, and the number of reads mapped with good mapping quality scores (MAPQ > 1) were determined with SAMtools (version 1.1.3; Li et al., 2009). Mapping quality scores indicates the confidence of alignments and uniqueness of the mapping position in the reference with higher values indicating a higher mapping quality. SAM to BAM format conversion was performed with SAMtools, excluding read alignments with a relatively low MAPQ smaller than 1 to maximize the number of mapped reads. Read duplicates were removed with PicardTools MarkDuplicates, and INDEL realignment was performed with GATK (version 3.1-1; McKenna et al., 2010) IndelRealigner to reduce the number of false-positive SNP calls. Resulting alignments were subjected to variant calling with GATK Unifiedgenotyper with a minimum confidence threshold for calling of 30.0 and for emitting of called SNPs of 10.0. Predicted SNP candidates were filtered with GATK Variantfiltration with following thresholds: FS > 30.0, QD < 2.0, MQRankSum < −12.5, ReadPosRankSum < −8.0. Filtered variants with a depth of coverage > 4 and a genotype quality > 30 were taken into consideration, and only homozygous SNPs were of interest in this study. Conserved domains were assigned to HC and LC genes using the NCBI Conserved Domain Database (Marchler-Bauer et al., 2015). The selected candidate was verified using Sanger sequencing on DNA obtained from 19 independent allelic *vrs3/int-a* mutants. The DNA was extracted from freeze-dried leaf material using the Qiagen BioSprint (Qiagen) according to manufacturer's protocol. Fragments for Sanger sequencing were amplified using the primers enlisted in Supplemental Table S6.

Transcriptional Profiling

For transcriptome analysis, we used a combined set of HC and LC predicted coding sequences of barley cv Morex (International Barley Genome Sequencing Consortium, 2012) as reference. Alignment of the reads to the reference was done using BWA-MEM using the same settings as applied for the variant calling. Transcripts per million values were extracted from the BWA-aligned reads using Salmon (Patro et al., 2017). Transcripts with expression levels greater than three counts in three libraries were retained. Tables with raw and normalized transcripts per million values and expression levels are provided as supplemental tables (Supplemental Tables S3 and S4). Differentially regulated reads were called using the R bioconductor package Limma-vroom using a Benjamin & Hochberg adjustment for multiple testing (false discovery rate) for calculation of the adjusted *P* values (FDR values; Ritchie et al., 2015). For expression analysis, an FDR value of 0.05 was used as initial cut-off value for the selection of DRTs. DRTs were extracted per mutant per developmental stage as well as the overall effect, which encompasses all transcripts affected in both W3.5 and W5.0 (Supplemental Fig. S4). Hierarchical cluster analysis was done in R using Pearson correlation coefficients. The overrepresentation analysis of particular GO terms was performed using the R-package TopGo (Alexa et al., 2006). All Venn diagrams were drawn using the R package VennDiagram (Chen and Boutros, 2011).

Results obtained for VRS1(AB259783.1), VRS3(MLOC_69611.1), VRS4 (KC854554), and INT-C(MLOC_70116.1) were verified by performing qRT-PCR using gene-specific primers (Supplemental Table S6). Primer sequences for Hv.ACTIN (AY145451), which was used as control, were used as previously described (Ejaz and von Korff, 2017); VRS4 primers were obtained from Koppolu et al. (2013). MSA tissue of cv Bowman and derived mutant lines *vrs3.f* and *vrs3 (int-a.1)* were harvested at the Waddington stages W2.0, W3.5, W4.0, W5.0, and W6.0 to analyze changes in the expression of *VRS1*, *VRS3*, *VRS4*, and *INT-C* during development. Samples were collected in three individual biological replicates. For each biological replicate, at least 10 MSA were pooled. In addition, MSA tissue was harvested in two to three biological replicates at W3.0 to W3.5 and W5.0 for *vrs1*, *vrs4*, *int-c vrs3.f*, and *vrs3*(*int-a.1)* mutants in cv Bowman; *vrs3*(*int-a.1)* and *vrs3(int-a.64)* in cv Bonus; and *vrs3(int-a.8)* in Foma background. The samples were harvested at the middle of the day, 6 to 8 h before the end of the light period. Before sampling, the developmental stage of the MSA was verified by dissecting three plants per genotype. RT-PCR and cDNA synthesis was performed as previously described (Ejaz and von Korff, 2017). Quantification was based on the titration curve for each target gene and normalized against *HvACTIN* as internal control using the LightCycler 480 Software (Roche; version 1.5). Statistical differences were either calculated with a Student's *t* test or a two-factorial ANOVA with genotype and stage as factors, followed by a post hoc Dunnett's test for multiple comparison.

Phylogenetic Analysis

The amino acid sequences of proteins annotated as JmjC domain-containing proteins from barley (*H. vulgare*), rice (*Oryza. sativa*), and Arabidopsis (*Arabidopsis thaliana*) were downloaded from the iTAK database 16.03 (Zheng et al., 2016). A multiple sequence alignment of the retrieved JmjC domain-containing proteins was performed using ClustalO with default parameters (Sievers et al., 2011). The resulting alignment was converted to Phylip format using Alter (Glez-Peña et al., 2010). RAxML 8.2.10 was used to generate a maximum likelihood tree with fixed base frequencies, the GAMMA model, and "autoMRE" as parameter to calculate the optimal number bootstrap repeats (Stamatakis et al., 2008). The automatically determined substitution model was chosen as the "VT" substitution model. The unrooted tree was visualized using Dendroscope 3 (Huson and Scornavacca, 2012), and classification into evolutionary conserved groups was manually performed according to Klose et al. (2006). The JmjC domains of the barley VRS3 protein, and the closest orthologs in rice (JMJ706) and Arabidopsis (JMJ13) were obtained from the NCBI conserved domain database (Marchler-Bauer and Bryant, 2004). ClustalO was used to align and to calculate the pairwise percent identity of the conserved JmjC domains of VRS3, Os.JMJ706, and At.JMJ13 with default settings (Sievers et al., 2011).

Supplemental Data

The following supplemental materials are available.

Supplemental Figure S1. Spike phenotypes of *vrs3*, *vrs1*, *vrs4*, and *int-c* in cv Bowman.

Supplemental Figure S2. Introgression locations of *vrs1*, *vrs4*, and *int-c* in cv Bowman.

Supplemental Figure S3. Phylogenetic relationship of proteins with JmjC domains.

Supplemental Figure S4. Differentially regulated transcripts in *vrs1*, *vrs3*, *int-a.1*, and *int-c.5*.

Supplemental Figure S5. Expression of *VRS3* compared to *INT-C* and *VRS1*.

Supplemental Figure S6. Expression of *VRS3* and *VRS4* determined with qRT-PCR.

Supplemental Table S1. Variants identified in independent *vrs3/int-a* mutants.

Supplemental Table S2. Percentage identity matrix and alignment of the jmjC domains of VRS3, Os.JMJ706, and At.JMJ13.

Supplemental Table S3. All transcripts expressed at W3.5 and W5.0.

Supplemental Table S4. Differentially regulated transcripts in *vrs1*, *vrs3(int-a.1)*, *vrs4.k*, and *int-c.5*.

Supplemental Table S5. GO overrepresentation analysis of genes differentially regulated in the row-type mutants.

Supplemental Table S6. Primers used for in this study.

Supplemental File S1. Variants_VRS3.vcf.

ACKNOWLEDGMENTS

We thank Caren Dawidson, Andrea Lossow, and Kerstin Luxa for excellent technical assistance in the laboratory and greenhouse. Artem Pankin is acknowledged for critically reading this manuscript and performing the phylogenetic analysis.

Received January 30, 2017; accepted June 25, 2017; published June 27, 2017.

LITERATURE CITED

Ahloowalia BS, Maluszynski M, Nichterlein K (2004) Global impact of mutation-derived varieties. Euphytica **135:** 187–204

Alexa A, Rahnenfuhrer J, Lengauer T (2006) Improved scoring of functional groups from gene expression data by decorrelating GO graph structure. Bioinformatics **22:** 1600–1607

Chen H, Boutros PC (2011) VennDiagram: a package for the generation of highly-customizable Venn and Euler diagrams in R. BMC Bioinformatics **12:** 35

Chen Q, Chen X, Wang Q, Zhang F, Lou Z, Zhang Q, Zhou DX (2013) Structural basis of a histone H3 lysine 4 demethylase required for stem elongation in rice. PLoS Genet **9:** e1003239

Cui X, Jin P, Cui X, Gu L, Lu Z, Xue Y, Wei L, Qi J, Song X, Luo M, An G, Cao X (2013) Control of transposon activity by a histone H3K4 demethylase in rice. Proc Natl Acad Sci USA **110:** 1953–1958

Druka A, Franckowiak J, Lundqvist U, Bonar N, Alexander J, Houston K, Radovic S, Shahinnia F, Vendramin V, Morgante M, Stein N, Waugh R (2011) Genetic dissection of barley morphology and development. Plant Physiol **155:** 617–627

Eisen MB, Spellman PT, Brown PO, Botstein D (1998) Cluster analysis and display of genome-wide expression patterns. Proc Natl Acad Sci USA **95:** 14863–14868

Ejaz M, von Korff M (2017) The genetic control of reproductive development under high ambient temperature. Plant Physiol **173:** 294–306

Gan ES, Xu Y, Wong JY, Goh JG, Sun B, Wee WY, Huang J, Ito T (2014) Jumonji demethylases moderate precocious flowering at elevated temperature via regulation of FLC in Arabidopsis. Nat Commun **5:** 5098

Grabherr MG, Haas BJ, Yassour M, Levin JZ, Thompson DA, Amit I, Adiconis X, Fan L, Raychowdhury R, Zeng Q, et al (2011) Trinity: reconstructing a full-length transcriptome without a genome from RNA-seq data. Nat Biotechnol **29:** 644–652

Gustafsson A, Lundqvist U (1980) Hexastichon and intermedium mutants in barley. Hereditas **92:** 229–236

Huson DH, Scornavacca C (2012) Dendroscope 3: an interactive tool for rooted phylogenetic trees and networks. Syst Biol **61:** 1061–1067

International Barley Genome Sequencing Consortium (2012) A physical, genetic and functional sequence assembly of the barley genome. Nature **491:** 711–716

James GV, Patel V, Nordström KJ, Klasen JR, Salomé PA, Weigel D, Schneeberger K (2013) User guide for mapping-by-sequencing in Arabidopsis. Genome Biol **14:** R61

Klose RJ, Kallin EM, Zhang Y (2006) JmjC-domain-containing proteins and histone demethylation. Nat Rev Genet **7:** 715–727

Komatsuda T, Pourkheirandish M, He C, Azhaguvel P, Kanamori H, Perovic D, Stein N, Graner A, Wicker T, Tagiri A, Lundqvist U, Fujimura T, et al (2007) Six-rowed barley originated from a mutation in a homeodomain-leucine zipper I-class homeobox gene. Proc Natl Acad Sci USA **104:** 1424–1429

Kooistra SM, Helin K (2012) Molecular mechanisms and potential functions of histone demethylases. Nat Rev Mol Cell Biol **13:** 297–311

Koppolu R, Anwar N, Sakuma S, Tagiri A, Lundqvist U, Pourkheirandish M, Rutten T, Seiler C, Himmelbach A, Ariyadasa R, Youssef HM, Stein N, et al (2013) Six-rowed spike4 (Vrs4) controls spikelet determinacy and row-type in barley. Proc Natl Acad Sci USA **110:** 13198–13203

Langmead B, Salzberg SL (2012) Fast gapped-read alignment with Bowtie 2. Nat Methods **9:** 357–359

Li H (2013) Aligning sequence reads, clone sequences and assembly contigs with BWA-MEM. arXiv 1303.3997

Li H, Handsaker B, Wysoker A, Fennell T, Ruan J, Homer N, Marth G, Abecasis G, Durbin R; 1000 Genome Project Data Processing Subgroup (2009) The Sequence Alignment/Map format and SAMtools. Bioinformatics **25:** 2078–2079

Liller CB, Neuhaus R, von Korff M, Koornneef M, van Esse W (2015) Mutations in barley row type genes have pleiotropic effects on shoot branching. PLoS One **10:** e0140246

Liller CB, Walla A, Boer MP, Hedley P, Macaulay M, Effgen S, von Korff M, van Esse GW, Koornneef M (2017) Fine mapping of a major QTL for awn length in barley using a multiparent mapping population. Theor Appl Genet **130:** 269–281

Liu C, Lu F, Cui X, Cao X (2010) Histone methylation in higher plants. Annu Rev Plant Biol **61:** 395–420

Lundqvist U (2014) Scandinavian mutation research in barley - a historical review. Hereditas **151:** 123–131

Lundqvist U, Abebe B, Lundqvist A (1988a) Gene interaction of induced intermedium mutations of two-row barley. II. Interaction between the *hex-v* gene and *int* genes. Hereditas **109:** 197–204

Lundqvist U, Abebe B, Lundqvist A (1988b) Gene interaction of induced intermedium mutations of two-row barley. III. Overlapping in dihybrid F2 classification patterns in combinations of recessive *int* genes. Hereditas **109:** 205–214

Lundqvist U, Lundqvist A (1987) An *intermedium* gene present in a commercial six-row variety of barley. Hereditas **107:** 131–135

Lundqvist U, Lundqvist A (1988a) Gene interaction of induced *intermedium* mutations of two-row barley. I. Double mutant recombinants. Hereditas **108:** 133–140

Lundqvist U, Lundqvist A (1988b) Induced *intermedium* mutants in barley: Origin, morphology and inheritance. Hereditas **108:** 13–26

Marchler-Bauer A, Bryant SH (2004) CD-Search: Protein domain annotations on the fly. Nucleic Acids Res **32:** W327–W331

Marchler-Bauer A, Derbyshire MK, Gonzales NR, Lu S, Chitsaz F, Geer LY, Geer RC, He J, Gwadz M, Hurwitz DI, Lanczycki CJ, Lu F, et al. (2015) CDD: NCBI's conserved domain database. Nucleic Acids Res **43:** D222–D226

Mayer KF, Waugh R, Brown JW, Schulman A, Langridge P, Platzer M, Fincher GB, Muehlbauer GJ, Sato K, Close TJ, Wise RP, Stein N; International Barley Genome Sequencing Consortium (2012) A physical, genetic and functional sequence assembly of the barley genome. Nature **491:** 711–716

McKenna A, Hanna M, Banks E, Sivachenko A, Cibulskis K, Kernytsky A, Garimella K, Altshuler D, Gabriel S, Daly M, DePristo MA (2010) The Genome Analysis Toolkit: a MapReduce framework for analyzing next-generation DNA sequencing data. Genome Res **20:** 1297–1303

Miura A, Nakamura M, Inagaki S, Kobayashi A, Saze H, Kakutani T (2009) An Arabidopsis jmjC domain protein protects transcribed genes from DNA methylation at CHG sites. EMBO J **28:** 1078–1086

Noh B, Lee SH, Kim HJ, Yi G, Shin EA, Lee M, Jung KJ, Doyle MR, Amasino RM, Noh YS (2004) Divergent roles of a pair of homologous jumonji/zinc-finger-class transcription factor proteins in the regulation of Arabidopsis flowering time. Plant Cell **16:** 2601–2613

Nordström KJ, Albani MC, James GV, Gutjahr C, Hartwig B, Turck F, Paszkowski U, Coupland G, Schneeberger K (2013) Mutation identification by direct comparison of whole-genome sequencing data from mutant and wild-type individuals using k-mers. Nat Biotechnol **31:** 325–330

Pankin A, Campoli C, Dong X, Kilian B, Sharma R, Himmelbach A, Saini R, Davis SJ, Stein N, Schneeberger K, von Korff M (2014) Mapping-by-sequencing identifies HvPHYTOCHROME C as a candidate gene for the early maturity 5 locus modulating the circadian clock and photoperiodic flowering in barley. Genetics **198:** 383–396

Patro R, Duggal G, Love MI, Irizarry RA, Kingsford C (2017) Salmon provides fast and bias-aware quantification of transcript expression. Nat Methods **14:** 417–419

Ramsay L, Comadran J, Druka A, Marshall DF, Thomas WT, Macaulay M, MacKenzie K, Simpson C, Fuller J, Bonar N, Hayes PM, Lundqvist U, et al. (2011) INTERMEDIUM-C, a modifier of lateral spikelet fertility in barley, is an ortholog of the maize domestication gene TEOSINTE BRANCHED 1. Nat Genet **43:** 169–172

Glez-Peña D, Gómez-Blanco D, Reboiro-Jato M, Fdez-Riverola F, Posada D (2010) ALTER: program-oriented conversion of DNA and protein alignments. Nucleic Acids Res **38:** W14-8

Ritchie ME, Phipson B, Wu D, Hu Y, Law CW, Shi W, Smyth GK (2015) *limma* powers differential expression analyses for RNA-sequencing and microarray studies. Nucleic Acids Res **43:** e47

Sakuma S, Pourkheirandish M, Hensel G, Kumlehn J, Stein N, Tagiri A, Yamaji N, Ma JF, Sassa H, Koba T, Komatsuda T (2013) Divergence of expression pattern contributed to neofunctionalization of duplicated HD-Zip I transcription factor in barley. New Phytol **197:** 939–948

Sánchez-Martín J, Steuernagel B, Ghosh S, Herren G, Hurni S, Adamski N, Vrána J, Kubaláková M, Krattinger SG, Wicker T, Doležel J, Keller B, et al (2016) Rapid gene isolation in barley and wheat by mutant chromosome sequencing. Genome Biol **17:** 221

Schneeberger K, Ossowski S, Lanz C, Juul T, Petersen AH, Nielsen KL, Jørgensen JE, Weigel D, Andersen SU (2009) SHOREmap: simultaneous mapping and mutation identification by deep sequencing. Nat Methods **6:** 550–551

Sievers F, Wilm A, Dineen D, Gibson TJ, Karplus K, Li W, Lopez R, McWilliam H, Remmert M, Söding J, Thompson JD, Higgins DG (2011) Fast, scalable generation of high-quality protein multiple sequence alignments using Clustal Omega. Mol Syst Biol **7:** 539

Searle IR, Pontes O, Melnyk CW, Smith LM, Baulcombe DC (2010) JMJ14, a JmjC domain protein, is required for RNA silencing and cell-to-cell movement of an RNA silencing signal in Arabidopsis. Genes Dev **24:** 986–991

Stamatakis A, Hoover P, Rougemont J (2008) A rapid bootstrap algorithm for the RAxML Web servers. Syst Biol **57:** 758–771

Steuernagel B, Periyannan SK, Hernández-Pinzón I, Witek K, Rouse MN, Yu G, Hatta A, Ayliffe M, Bariana H, Jones JD, Lagudah ES, Wulff BB (2016) Rapid cloning of disease-resistance genes in plants using mutagenesis and sequence capture. Nat Biotechnol **34:** 652–655

Studer AJ, Doebley JF (2011) Do large effect QTL fractionate? A case study at the maize domestication QTL teosinte branched1. Genetics **188:** 673–681

Studer A, Zhao Q, Ross-Ibarra J, Doebley J (2011) Identification of a functional transposon insertion in the maize domestication gene tb1. Nat Genet **43:** 1160–1163

Sun Q, Zhou DX (2008) Rice jmjC domain-containing gene JMJ706 encodes H3K9 demethylase required for floral organ development. Proc Natl Acad Sci USA **105:** 13679–13684

Trick M, Adamski NM, Mugford SG, Jiang CC, Febrer M, Uauy C (2012) Combining SNP discovery from next-generation sequencing data with bulked segregant analysis (BSA) to fine-map genes in polyploid wheat. BMC Plant Biol **12:** 14

Waddington SR, Cartwright PM, Wall PC (1983) A quantitative scale of spike initial and pistil development in barley and wheat. Ann Bot **51:** 119–130

Whipple CJ, Kebrom TH, Weber AL, Yang F, Hall D, Meeley R, Schmidt R, Doebley J, Brutnell TP, Jackson DP (2011) *grassy tillers1* promotes apical dominance in maize and responds to shade signals in the grasses. Proc Natl Acad Sci USA **108:** E506–E512

Yu X, Li L, Li L, Guo M, Chory J, Yin Y (2008) Modulation of brassinosteroid-regulated gene expression by Jumonji domain-containing proteins ELF6 and REF6 in Arabidopsis. Proc Natl Acad Sci USA **105:** 7618–7623

Zheng Y, Jiao C, Sun H, Rosli HG, Pombo MA, Zhang P, Banf M, Dai X, Martin GB, Giovannoni JJ, Zhao PX, Rhee SY, et al. (2016) iTAK: A program for genome-wide prediction and classification of plant transcription factors, transcriptional regulators, and protein kinases. Mol Plant **9:** 1667–1670